

# Pelletisation by tumbling as an alternative method of agglomerating nanometric particles for use as feedstock in bi-modal structured flame-sprayed ceramic coatings



Jhoman Alberto Arias<sup>a</sup>, Francy Milena Hurtado<sup>a</sup>, Freddy Vargas<sup>b</sup>, Geraldine Estrada<sup>a</sup>, Edwin Cadavid<sup>a</sup>, Mauricio Rincón Ortiz<sup>b,\*</sup>, Claudia Constanza Palacio<sup>c</sup>, Fabio Vargas<sup>a</sup>

<sup>a</sup> GIPIMME and GIMACYR, Universidad de Antioquia, Street 67 # 53-108, 050010, Medellín, Colombia

<sup>b</sup> Grupo de Investigación en Desarrollo y Tecnología de Nuevos Materiales – Universidad Industrial de Santander UIS, 680002, Cr 27 Calle 9, Bucaramanga, Santander, Colombia

<sup>c</sup> Universidad EAFIT, GEMA, Cra 49 # 7s-50, 050010, Medellín, Colombia

## ARTICLE INFO

### Keywords:

Pelletisation  
Nanoparticles  
Thermally sprayed coatings  
Bi-modal structure

## ABSTRACT

This paper is focused on the physical evaluation of ceramic granules of Al<sub>2</sub>O<sub>3</sub>, Al<sub>2</sub>O<sub>3</sub>-13 wt% TiO<sub>2</sub> (AT-13) and TiO<sub>2</sub> obtained from alumina and titania nanoparticles by pelletisation in a rotating drum. The results were compared with those of both sintered and non-sintered granules of similar chemical compositions and particle size distributions which were spray dried, as well as with those of TiO<sub>2</sub> pelletised granules blended with atomised alumina particles. The results obtained indicated that the physical characteristics of the pelletised granules conferred them a free-flowing behavior which was similar to that of the spray-dried granules. However, the TiO<sub>2</sub> pelletised granules blended with harder atomised alumina particles disintegrated and, therefore, exhibited a poor flowability. Additionally, it was evident that the ceramic coatings fabricated from pelletised granules displayed a structure which was as or more compact than those of the granules obtained from agglomerated powders by spray drying with or without sintering, apart from being more compact than that of the coatings deposited from TiO<sub>2</sub> pelletised granules blended with atomised alumina particles. The above findings indicate that the alternative pelletising method is potentially useful for the use of agglomerated nanoparticles as feedstock in the fabrication of bi-modal structured flame-sprayed ceramic coatings.

## 1. Introduction

Bi-modal structured thermally sprayed ceramic coatings, fabricated from either nanometric or submicrometric agglomerated particles, are being widely used to protect metallic substrates owing to their good performances in demanding mechanical and thermal conditions and in biomedical and environmental applications, among others [1–5].

Nanometric or submicrometric agglomerated powders, which are commercially available for thermal spraying, are mainly granulated by spray drying process [6–8] owing to the ability to meet the requirements for particle size distribution, which typically must be between 10 and 110 μm, and the obtention of smooth surfaces and spherical shapes, which result in a great flow capacity, which is important for the fabrication of structurally homogeneous coatings [1,9,10].

In the spray drying process, an aqueous suspension of nanometric or submicrometric particles containing a binder is atomised through a

nozzle, which allows control of the size, distribution, trajectory and speed of the drops. Furthermore, it is possible to control the energy required to form an aerosol according to the size distribution and the content of starting particles in the suspension, as well as by the feed rate. Each drop which is constituted by water, particles and binder is exposed to a hot air flow in a drying chamber, where the heat required to evaporate the liquid is supplied; the hot air drags the dry particles with it towards the classifier cyclone. Thanks to the interactions between the particles in the drying chamber (collisions, electrostatic effects and the effect of the added binder), the formation of agglomerated materials with different morphologies and particle size distributions is achieved. Subsequently, the agglomerated particles are transported to the classifier cyclone, wherein the bigger particles fall into a collector cup located at the bottom. Finally, the finer particles are dragged upwards through the gas exhaust pipe to a filter, where they are collected [11–19]. The morphology and size distribution of the agglomerated

\* Corresponding author. Carrera 28 # 33-84 Apt. 1604, Bucaramanga, Colombia.  
E-mail address: [mrinconosaber@uis.edu.co](mailto:mrinconosaber@uis.edu.co) (M. Rincón Ortiz).

particles depend, among other parameters, on the content of solids in the aqueous suspension. The maximum content of micrometric particles in a fluid suspension is 40–50 vol%, however, for nanometric particles, this content is generally 10–15 vol% [20–22], which leads to a high water consumption, as well as to a high consumption of the energy used to dry the suspension. Owing to the friability of the granules obtained by spray drying, they are frequently sintered to avoid fracturing during their manipulation or transport [1,23].

On the other hand, tumble or growth agglomeration (also called pelletisation) is performed in inclined discs (pans) or rotating drums. It is widely used in mineral processing and fertiliser granulation in order to obtain high-density “balls” or pellets with a granule size distribution of 2–20 mm by means of the tumbling action caused by the balance between gravity and centrifugal forces [24]. Agglomeration is realised by the natural adhesion of individual particles to each other being improved by the addition of binders, and is controlled by the competition between volume-related separation and surface-related adhesion forces. The last ones act only over short ranges, therefore, the adhesion tendency increases with decreasing particle size. The particle size distribution of starting powders used to achieve agglomeration by tumbling is typically between 100 and 200  $\mu\text{m}$  [25–28]. The viscosity of the liquid binder, as well as the size of the drops and their volumetric ratio relative to the solid phase, determine the wettability of the particles and, subsequently, the consolidation and growth of granules. Binders exhibiting a high viscosity are atomised in large drops, resulting in a higher degree of granulation for a given solution to solid phase ratio [29]. Hence, the conventional tumbling granulation is not suitable for producing very small granules [24], since large drops of the binder produce big granulates, which are typically of the order of millimetres.

In this study, a nozzle developed by the University of Antioquia-Colombia was used to spray a binder in a rotating drum in order to agglomerate nanoparticles by an alternative pelletisation method. The granules obtained were used as feedstock material to fabricate bi-modal structured thermally sprayed coatings. The coatings obtained were compared with those sprayed from sintered and non-sintered granules which were spray dried, as well as with that fabricated from  $\text{Al}_2\text{O}_3$ -13 wt%  $\text{TiO}_2$  (AT-13) powder, which contains alumina atomised microparticles and  $\text{TiO}_2$  pelletised granules.

## 2. Materials and methods

### 2.1. Feedstock powders

The alumina and titania powders fabricated by US Research Nanomaterials Inc, with average particle sizes of 80 and 18 nm, respectively, were agglomerated in the laboratory by using both the alternative pelletisation method and the conventional spray drying process in order to obtain  $\text{Al}_2\text{O}_3$ , AT-13 and  $\text{TiO}_2$  granules. The size distributions of the  $\text{Al}_2\text{O}_3$  and AT-13 granules were  $d_{10} > 5 \mu\text{m}$  and  $d_{90} < 75 \mu\text{m}$ , whereas that of the agglomerated  $\text{TiO}_2$  was  $d_{10} > 15 \mu\text{m}$  and  $d_{90} < 95 \mu\text{m}$ . Prior to the agglomeration process, the alumina and titania nanoparticles were mechanically mixed in a rotating drum at 60 rpm for one hour to achieve a homogeneous distribution of the AT-13 composition.

Furthermore, the commercial alumina microparticles manufactured by Oerlikon Metco, namely SFP 105™, were atomised in an oxy-fuel flame and subsequently blended with 13 wt%  $\text{TiO}_2$  powder which was agglomerated in the laboratory by pelletisation method.

The Oerlikon Metco, SFP 105™  $\text{Al}_2\text{O}_3$  powder was atomised in order to obtain spherical particles with good flowability and was subsequently blended with pelletised  $\text{TiO}_2$  granules to evaluate the mechanical resistance of the titania agglomerates when they are in contact with the harder alumina particles.

The powders produced in the laboratory, as well as those commercially fabricated by Oerlikon Metco, namely 6103™, 6221™ and 6231A™, which correspond to  $\text{Al}_2\text{O}_3$ , AT-13 and  $\text{TiO}_2$ , respectively,

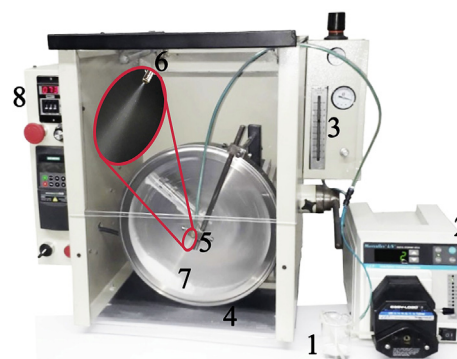


Fig. 1. Pelletisation device. 1. Binder solution, 2. Peristaltic pump, 3. Flow and pressure of air control box, 4. Drum, 5. Nozzle, 6. Nozzle detail, 7. Powder, 8. Time and drum speed control box.

were used to fabricate flame-sprayed coatings. These Oerlikon Metco powders were prepared by spray drying and sintering.

### 2.2. Agglomeration processes

#### 2.2.1. Pelletisation

An alternative pelletisation method was used to agglomerate nanoparticles in a rotating drum, which was equipped with a binder feeder system which comprised a peristaltic pump Masterflex® L/S®, coaxial hoses and a nozzle. An aqueous solution of the binder was pumped to the nozzle through the internal hose, while a stream of compressed air at a low flow rate and high pressure was injected through the external hose. The binder solution and the stream of compressed air were ejected through a hole in the nozzle which was 426  $\mu\text{m}$  in diameter to produce micrometric droplets (Fig. 1).

Prior to the pelletisation process, the viscosity and wettability of the aqueous binder solutions with different weight percentages of polyvinyl alcohol were measured; these solutions were then pumped and sprayed using the feeder system of the equipment in order to determine which of them can be atomised to produce a fog. The viscosity was measured according to ASTM D1200 standard [30], while the wettability tests were performed by measuring the contact angle of the binder solution droplets on the pressed bar made of each powder. The most appropriate solution for producing a binder fog and agglomerating the nanoparticles was a blend of 2.3 wt% polyvinyl alcohol in water, the viscosity of which was  $\approx 20$  cSt, and its contact angle on the bar surfaces varied between 40° and 45°.

Agglomeration tests were previously carried out to establish the most adequate parameters for obtaining granules with the particle size distribution indicated above. Better granules were obtained by feeding 15 g of powder into the drum, which was subsequently rotated at 80 rpm in order to produce a cascading motion of the particles. Subsequently, the following were pumped through the internal hose of the feeder system: 5.45 ml of the binder solution for  $\text{Al}_2\text{O}_3$ , 8.18 ml for AT-13 and 15 ml for  $\text{TiO}_2$  at a flow rate of 2 ml/min. Simultaneously, a compressed air stream of 0.1 MPa and 2.8 l/min was injected into the nozzle through the external hose, which produced a binder fog which wetted the surface of the particles; the volumetric percentages of the solids reached  $\approx 41\%$  for  $\text{Al}_2\text{O}_3$ ,  $\approx 32\%$  for AT-13 and  $\approx 20\%$  for  $\text{TiO}_2$ . The granules obtained were dried at room temperature for 24 h and then sieved.

#### 2.2.2. Spray drying process

A Toption TP S-15™ spray dryer (Fig. 2) was used to agglomerate the nanoparticles in an aqueous solution to form different slurries composed of 2 wt% polyvinyl alcohol as the binder, 0.5 wt% of polyacrylic dispersant as the deflocculant and the particles. Each slurry contained a different quantity of particles: the  $\text{Al}_2\text{O}_3$  slurry contained 30 wt%



Fig. 2. Image of Toption TP S-15™ spray dryer. 1. Slurry, 2. Peristaltic pump, 3. Slurry inlet to the nozzle, 4. Nozzle detail, 5. Drying chamber, 6. Collector cup, 7. Classifier cyclone, 8. Exhaust pipe, 9. Control panel

(10 vol %) of powder; the AT-13 slurry, 20 wt% (6 vol %) of powder; and the TiO<sub>2</sub> slurry, 10 wt% (2.8 vol %) of powder. During the agglomeration process, a peristaltic pump pumped the slurries to the drying chamber at the flow rates of 7.3, 6.96 and 3.1 ml/min for Al<sub>2</sub>O<sub>3</sub>, AT-13 and TiO<sub>2</sub>, respectively. Subsequently, each slurry was atomised by an air stream of 0.1 MPa pressure through a nozzle located in the upper part of the chamber, the spraying hole of which was 1 mm in diameter (Fig. 2). Each atomised drop (constituted by a mixture of water, particles, deflocculant and binder), was exposed to flowing hot air, which heats the drying chamber to 220 °C and evaporates the water and deflocculant. The interactions among the nanoparticles in the drying chamber promoted the formation of granules, which were dragged towards the cyclone classifier. The heaviest particles fall into the collector cup located at the bottom of the cyclone, while the lightest particles were dragged upwards through the gas exhaust pipe to a filter, where they were collected (Fig. 2). Finally, the spray-dried granules collected in the collector cup, as well as those bonded to the wall of the drying chamber, were sieved to obtain granules with the particle size distribution indicated above.

The spray drying parameters were established from the preliminary tests carried out to obtain granules which are suitable for the fabrication of coatings by flame spraying process.

Table 1  
Flame spraying parameters.

| Spraying parameters                  | Powders        |                    |                |                |                    |                |                |                    |                |                    |
|--------------------------------------|----------------|--------------------|----------------|----------------|--------------------|----------------|----------------|--------------------|----------------|--------------------|
|                                      | Pelletised     |                    |                | Spray dried    |                    |                | Commercial     |                    | Blended        |                    |
|                                      | A <sub>p</sub> | AT-13 <sub>p</sub> | T <sub>p</sub> | A <sub>s</sub> | AT-13 <sub>s</sub> | T <sub>s</sub> | A <sub>c</sub> | AT-13 <sub>c</sub> | T <sub>c</sub> | AT-13 <sub>b</sub> |
| Acetylene [L/min]                    |                |                    |                |                |                    | 22             |                |                    |                |                    |
| Oxygen [L/min]                       |                | 70                 | 55             | 75             | 70                 | 55             | 75             | 70                 | 55             | 70                 |
| Substrate material                   |                | AISI 1020          | Clay Brick     | AISI 1020      |                    | Clay Brick     | AISI 1020      |                    | Clay Brick     | AISI 1020          |
| Preheating passes                    | 3              | 3                  | 4              | 3              | 3                  | 4              | 3              | 3                  | 4              | 3                  |
| Spraying passes                      | 8              | 6                  | 6              | 10             | 6                  | 6              | 7              | 8                  | 6              | 8                  |
| Rotational speed of substrates [rpm] | 116            | 127                | 127            | 127            | 127                | 127            | 46.1           | 116                | 127            | 116                |
| Linear speed [cm/s]                  | 0.56           | 0.51               | 0.67           | 0.51           | 0.51               | 0.67           | 0.29           | 0.59               | 0.67           | 0.59               |
| Spraying distance [mm]               |                |                    |                |                |                    | 90             |                |                    |                |                    |
| Powder flow rate [g/min]             | 9              | 9                  | 9.6            | 10.8           | 9                  | 7.2            | 9              | 9                  | 9.6            | 6                  |

### 2.3. Characterisation of the agglomerated powders

The morphology of the agglomerates obtained in the laboratory by pelletisation and spray drying methods, as well as of those fabricated from Oerlikon Metco 6103™, 6221™ and 6231A™, was analysed by scanning electron microscopy (SEM), which was carried out using JEOL JSM-6490LV equipment. Additionally, the particle size distribution was determined from the SEM images by using Image J software.

Considering that the flowability of the feedstock powders in the thermal spraying equipment used to fabricate the coatings is based on Hausner ratio, this parameter was determined for the particles agglomerated in the laboratory, as well as for those of Oerlikon Metco.

### 2.4. Fabrication and characterisation of the coatings

The particles agglomerated in the laboratory, as well as those fabricated by Oerlikon Metco 6103™, 6221™ and 6231A™, were used as the feedstock powders for obtaining flame-sprayed coatings by using an electromechanical chamber, which was equipped with a Castolin Eutectic Terodyn 2000™ torch. This chamber was fabricated by the University of Antioquia-Colombia and allows control of the flow rates of the powders, the combustion and powder feed gases, the spraying speed, and the spraying distance; it also measures the preheating temperature of the substrate, among other spraying parameters.

In order to identify the coating samples, they were codified according to the chemical composition and powder preparation process, as follow. A was used to denote Al<sub>2</sub>O<sub>3</sub>; AT-13, Al<sub>2</sub>O<sub>3</sub>-13 wt% TiO<sub>2</sub>; and T, TiO<sub>2</sub>. Additionally, the subscript p was added to denote the pelletised powders, s to denote the spray-dried powders, c to indicate commercial and b to represent blended. The coatings were fabricated based on the thermal spraying parameters listed in Table 1, which were determined from previous experiments, the purpose of which was to obtain coatings with a bi-modal structure.

The flame used to fabricate the coatings was produced by feeding to the torch mixtures of acetylene and oxygen (indicated in Table 1), with the pressures of 0.08 and 0.34 MPa, respectively. The substrates were preheated by passing the flame in front of them, as indicated in Table 1. Afterwards, the feedstock powder was injected into the flame by using a nitrogen stream of 17 l/min at a pressure of 0.27 MPa as the carrier gas. During the spraying process, the substrates (bars 25 mm in diameter and 6 mm in length of both AISI 1020 and clay brick) were placed in front of the torch at the spraying distance indicated in Table 1 and then were rotated at the speed listed in the table. Finally, the torch was passed in front of the substrates, which resulted in spraying of the feedstock powders at a linear speed for the number of spraying passes shown in Table 1.

The substrate on which each coating was deposited was selected according to its potential application. The alumina and AT-13 coatings are generally used to protect steels exposed to tribological effects,

whereas those of TiO<sub>2</sub> on clay bricks can be used in photocatalytic applications.

The enthalpy of the flame used to fabricate the coatings was calculated using the Jets&Poudres software, based on the spraying parameters shown in Table 1.

The structures of the coatings were analysed at their cross sections by using SEM; the cross sections were obtained after mounting the samples with an epoxy resin and cutting with a diamond blade. Finally, the samples were grinded and polished according to ASTM E1920 standard [31].

On the other hand, the Vickers microhardness was measured on the polished surface of each coating according to ASTM C1327-15 [32] by using a Shimadzu G20 series tester. Taking into account the results reported by other authors, Weibull analysis was carried out to identify how the changes in the hardness of the coatings are related to their bimodal structure [33–35].

### 3. Results and discussion

#### 3.1. Morphology and flowability of the agglomerated powders

SEM observations allowed us to establish the idea that all the powders are constituted of particles with micrometric size distributions, as shown in Table 2 and Figs. 3–6. Additionally, it was evident that all these granules are highly spheroidised, except those of the TiO<sub>2</sub> pelletised and spray dried in the laboratory. Furthermore, the agglomerates obtained by pelletisation (Fig. 3 b), d), f)) are more compact than those obtained by spray drying without sintering (Fig. 4 b), d), f)), and it was evident that, as the size of the granulates increases, the agglomerates become more compact, especially of those pelletised. The higher compaction of the pelletised granules is owing to the better packaging of particles when they rotate and move on a solid surface such as the drum wall, compared to when they are dragged in a gas stream, as in the spray drying process. Other authors have indicated that tumbling granulators are good for producing high-density “balls” or pellets [24].

Furthermore, blowholes were evidenced in some of the particles spray dried in the laboratory which were not sintered, as observed in Fig. 4 b), d), f). Others authors have indicated that the highly porous and permeable structure in spray-dried granules, allows the flow of water vapour and possibly dissolved gases from the interior of the agglomerate to its surface, which produces blowholes [36].

For its part, the AT-13 blended powder is constituted by solid and spherical alumina particles ( $d_{10} = 4 \mu\text{m}$  and  $d_{90} = 21 \mu\text{m}$ ) and nano-agglomerated titania particles ( $d_{10} = 5 \mu\text{m}$  and  $d_{90} = 15 \mu\text{m}$ ). The TiO<sub>2</sub> granules were disintegrated at the contact with Al<sub>2</sub>O<sub>3</sub> during the mixing and transport processes, which resulted in small and irregular shaped granules of titania, whereas the size and shape of the alumina particles did not show appreciable changes (Fig. 5).

Regarding the Oerlikon Metco 6103™, 6221™ and 6231A™ commercial powders, it was evident that they were more spherical than the powders spray dried in the laboratory (Fig. 6). Besides, sintering necks grew among some of the submicrometric particles constituting these powders, which rendered them highly cohesive (Fig. 6 b), d), f)). Other authors have indicated that in the AT-13 granules spray dried from nanoparticle suspensions (10–20 nm for Al<sub>2</sub>O<sub>3</sub> and 20–30 nm for TiO<sub>2</sub>)

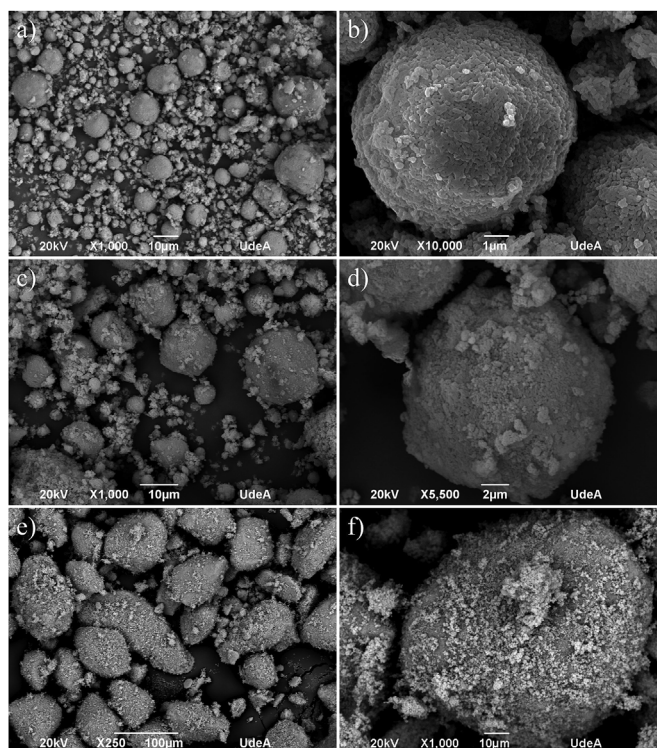


Fig. 3. The granules obtained from pelletised nanometric particles: a) and b) Alumina (A<sub>p</sub>), c) and d) AT-13<sub>p</sub>, e) and f) Titania (T<sub>p</sub>).

and subsequently sintered at 1350 °C, the constituent particles are of submicrometric size. The growth of nanoparticles to submicrometric sizes is due to the bonding of the agglomerated particles during sintering process [37]. Additionally, some of 6221™ and 6231A™ contain blowholes, which confer them a donut shape.

The size and geometry of the particles in a powder affect its flowability, since they influence the inter-particulate interactions. Hausner ratio predicts the propensity of a given powder sample to be compressed. This parameter is used to express flowability, since it reflects the importance of inter-particulate interactions. These interactions are generally less significant for a free-flowing powder, for which the bulk and tapped densities will be relative close in magnitude [38,39]. It is important to note that the Hausner ratio for a free-flowing powder is lower than 1.25 [37,40] and that an increase beyond this value represents a reduction in its flowability. The Hausner ratios measured for the granules obtained by pelletisation and spray drying, as well as for the commercially available Oerlikon-Metco 6103™, 6221™ and 6231A™, are between 1.10 and 1.18, whereas it is 1.32 for the AT-13 blended powder; see Table 2.

The aforementioned results indicate that the bulk and tapped densities of the granules processed in the laboratory by pelletisation and spray drying without sintering, as well as those of the Oerlikon-Metco 6103™, 6221™ and 6231A™ spray-dried and sintered powders, are relatively close in magnitude. Further, these powders can be considered

Table 2  
Particle size distribution and Hausner ratio for agglomerated powders.

| Property   | Powders        |                    |                |                |                    |                |                |                    |                |                    |
|--|----------------|--------------------|----------------|----------------|--------------------|----------------|----------------|--------------------|----------------|--------------------|
|  | Pelletised     |                    |                | Spray dried    |                    |                |                | Commercial         |                | Blended            |
|  | A <sub>p</sub> | AT-13 <sub>p</sub> | T <sub>p</sub> | A <sub>s</sub> | AT-13 <sub>s</sub> | T <sub>s</sub> | A <sub>c</sub> | AT-13 <sub>c</sub> | T <sub>c</sub> | AT-13 <sub>b</sub> |
| Particle size distribution $d_{10}/d_{90}$ ( $\mu\text{m}$ ) | 6/40           | 10/40              | 15/92          | 12/37          | 5/24               | 33/81          | 7/41           | 8/37               | 45/94          | 4/21               |
| Hausner ratio  | 1.10           | 1.18               | 1.15           | 1.08           | 1.16               | 1.06           | 1.09           | 1.05               | 1.13           | 1.32               |

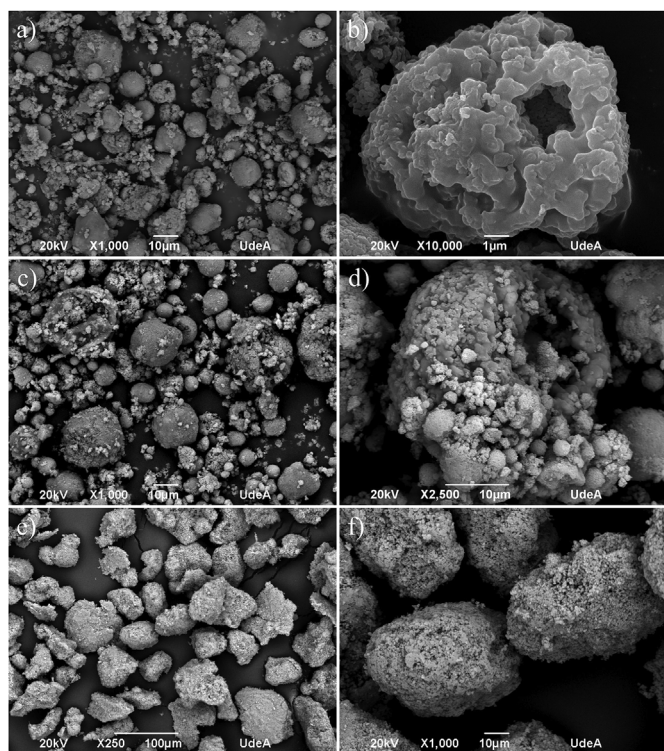


Fig. 4. The granules obtained from spray-dried nanometric particles: a) and b) Alumina (A<sub>s</sub>), c) and d) AT-13, e) and f) Titania (T<sub>s</sub>).

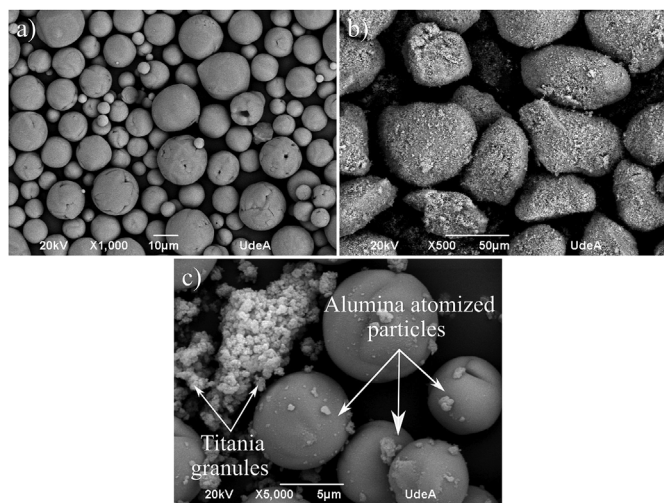


Fig. 5. The Particles constituting AT-13 blended powder. a) Atomised Al<sub>2</sub>O<sub>3</sub> particles, b) granules of TiO<sub>2</sub> pelletised (T<sub>p</sub>), c) AT-13 blended powder (AT-13<sub>b</sub>).

as free-flowing, since their Hausner ratios are lower than 1.25. However, it is important to note that the powders agglomerated in the laboratory by pelletisation and spray drying were not sintered and, consequently, they could be more friable than those commercially available, which were manufactured by spray drying and sintering.

On the other hand, although the alumina atomised particles can be considered as free-flowing owing to the Hausner ratio being 1.14, the Hausner ratio of the AT-13 blended powder is 1.32, which suggests a poor flowability which is attributed to the small size of TiO<sub>2</sub> granules disintegrate, as well as to their irregular shape.

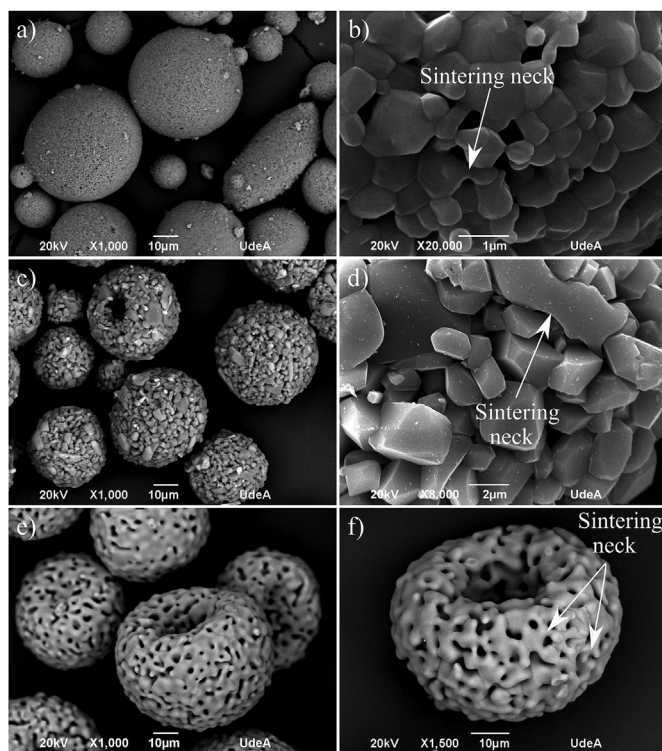


Fig. 6. Oerlikon-Metco powders a) and b) 6103™, c) and d) 6221™ and e) and f) 6231A™.

### 3.2. Structure of the coatings

The SEM images indicated that the structure of the alumina coatings sprayed from powders contains fully melted lamellae (FML), cracks, voids or pores, as well as partially melted particles (PMP) and partially melted lamellae (PML), which are characteristic of thermally sprayed coatings [1,2,19,41,42]. In coatings fabricated from agglomerated powders, the PMP and PML retain the fine particles which constitute the feedstock granules, which determine the bi-modal structure [1,2].

It was possible to establish that, in the alumina coatings, the structure of the A<sub>c</sub> sample is highly porous and formed by the stacking of a large number of PMP. These PML preserve the spherical shape of the granules used as the feedstock and the submicrometric particles that constitute them (Fig. 7a) and b)). On the other hand, the structures of A<sub>s</sub> and A<sub>p</sub> coatings are more compact than that of A<sub>c</sub> coating, and they are constituted stacked lamellae, some of which are partially melted (PML). These PML are composed of the nanometric particles used to prepare the granules employed as feedstock to spray the coatings (Fig. 7c) and d), e), f)).

Additionally, it was evident that the fine particles in the PML of the A<sub>p</sub> and A<sub>s</sub> coatings are larger than those constituting the granules used as feedstock in the fabrication of these samples (Figs. 3 b), 4 b) and 7d), f)). Moreover, it was observed that the quantity of PML in the A<sub>p</sub> coating is higher than that in the A<sub>s</sub> sample. It should be noted that some of the fine particles that constitute the PML in the A<sub>s</sub> coating were detached by the electron beam used during the SEM analysis (Fig. 7 d)).

The large quantity of the PMP which constitute the A<sub>c</sub> sample and the high porosity of its structure can be explained by the inability of the oxy-fuel flame to melt the submicrometric alumina particles, which constitute the granules used as feedstock in the fabrication of this coating.

A previous study has indicated that the hottest zone of the oxyacetylene flame produced from a mixture similar to that used to fabricate this coating displays a length close to 85 mm and a temperature which reaches 2180 °C [43], which is higher than the melting point of Al<sub>2</sub>O<sub>3</sub>

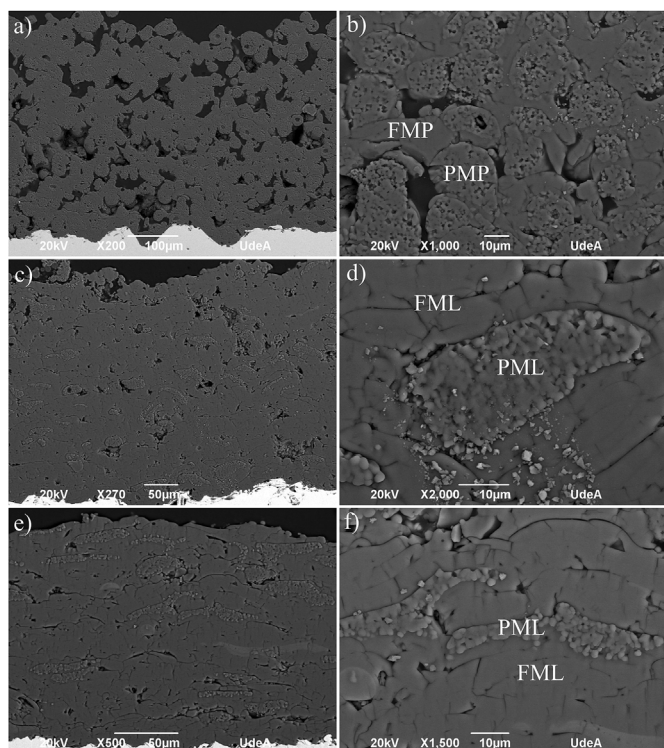


**Fig. 7.** Structure of the alumina coatings fabricated from different powders. a) and b) Oerlikon-Metco 6103™ spray-dried and sintered, c) and d) Spray-dried in the laboratory without sintering, e) and f) Pelletised in laboratory without sintering.

( $\approx 2047^\circ\text{C}$ ) [44]. However, this flame is not enough to completely melt the submicrometric alumina particles, since their residence time in the flame is only 1.5 ms for particles traveling at 60 m/s across 90 mm spraying distance, which is a typical speed for this process.

The enthalpies of the flames used to spray the coatings from pelletised and spray-dried granules were 5739 and 6067 J/s, respectively. The energies of these flames were sufficient to melt the pelletised and spray-dried granules, which were not sintered, but insufficient to melt the spray-dried and sintered granules manufactured by Oerlikon Metco. These results indicate that the growth of the particles which constitute the spray-dried granules during the sintering process makes it difficult to melt them.

Additionally, the more compact structure of pelletised granules facilitates the sintering of fine particles that constitute them, during their flight in the flame, which increases their cohesion and the size of the fine particles remaining in the PML of the  $A_p$  coating.

On the other hand, it was evident that the fine particles constituting the PML of the coating sprayed from granules spray dried without sintering were not sufficiently sintered to resist the energy applied by the electron beam during the SEM analysis, which resulted in their detachment from the coating; see Fig. 7 d). This was due to the large distance between particles which were not highly agglomerated or compacted.

Similar to those of the alumina samples, the structure of the AT-13 coatings is constituted by FML, PML, PMP, pores or voids and cracks, which are characteristic of bi-modal structured thermally sprayed coatings [1,2].

Furthermore, the SEM analysis allowed us to establish the fact that the addition of 13 wt%  $\text{TiO}_2$  to  $\text{Al}_2\text{O}_3$  to achieve agglomeration improves the melting of the granules used as feedstock in spraying the coatings.

From the above findings, the structure of the AT-13 coatings is composed of lamellae with a good stacking, even in the coating

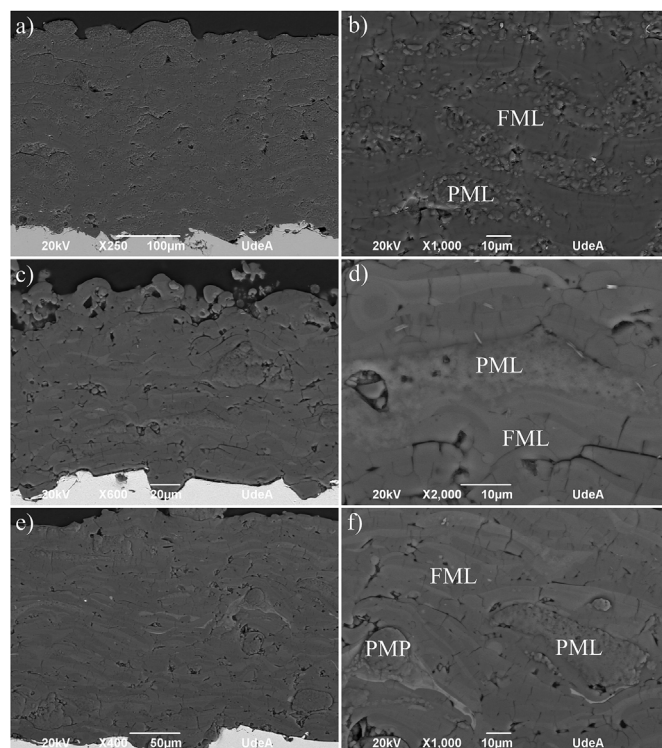


**Fig. 8.** Structure of AT-13 coatings fabricated from different powders. a) and b) Oerlikon-Metco 6221™ spray-dried and sintered, c) and d) Spray dried in the laboratory without sintering, e) and f) pelletised in laboratory without sintering.

fabricated from the spray-dried and sintered granules of Oerlikon-Metco 6221™, which is constituted by submicrometric particles, which can be harder to melt in the flame (Fig. 8). The improved melting of granules with the addition of  $\text{TiO}_2$  to  $\text{Al}_2\text{O}_3$  is owing to the lower melting point of titania ( $\approx 1840^\circ\text{C}$ ) [45] compared with that of alumina ( $\approx 2047^\circ\text{C}$ ) [44].

Additionally, it was evident that the quantity of PML (which retain the fine particles that constitute the granules used to fabricate the coatings) in the structure of AT-13c coating is higher than those in AT-13p and AT-13s. This is because AT-13c was thermally sprayed from granules composed of submicrometric particles, whereas AT-13p and AT-13s coatings were fabricated from granules shaped by nanoparticles, being the last ones easier to melt completely.

Furthermore, the fine particles in the PML of these three coatings remained well bonded together and no detachment due to the electron beam was observed during the SEM analysis, which indicated that these particles were sufficiently sintered during the formation of the coating (Fig. 8 b), d), f). The improvement in the sintering of the fine particles in the PML of AT-13 coatings relative to that of the alumina samples was attributed to the lowering of the melting point upon the addition of  $\text{TiO}_2$  and the consequent increase in the mobility of atoms during the heating of the particles during the thermal spray process.

For its part, the structure of the AT-13 coating fabricated from alumina atomised particles blended with  $\text{TiO}_2$  granules is constituted by lamellae, pores, cracks and PMP; the PMP are mainly of alumina. In contrast, the small amount of  $\text{TiO}_2$  PMP which retain the fine particles in the coating structure is attributable to both the low melting temperature of titania and the small size of the granules obtained after their disintegration at the contact with the atomised alumina powder. Therefore, this sample can be considered as a conventional mono-modal coating.

The above findings indicate that the enthalpy of the flame (5739 J/s) used to fabricate this coating is excessive for retaining the fine titania

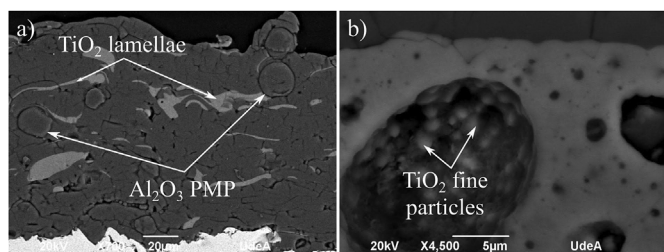


Fig. 9. Structure of Al<sub>2</sub>O<sub>3</sub>-13 wt% TiO<sub>2</sub> coatings fabricated from blended powders.

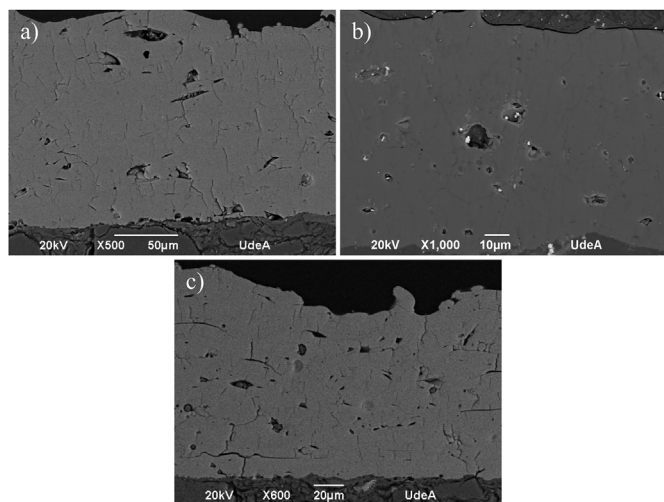


Fig. 10. Structure of TiO<sub>2</sub> coatings fabricated from different agglomerated powders. a) Oerlikon-Metco 6231A™ spray-dried and sintered, b) Spray-dried in the laboratory without sintering and c) pelletised in laboratory without sintering.

particles in its structure, nevertheless, a flame with a lower enthalpy (5223 J/s) was not used because it could not melt the atomised alumina particles. Furthermore, the low thickness of this coating, which was caused by the low flowability of the feedstock powder, which hindered its continuous supply during the thermal spraying process, is evident (Fig. 9a) and b)).

SEM analysis of the TiO<sub>2</sub> samples allowed us to establish that the structure is constituted by lamellae, pores and cracks, which are characteristic of conventional thermally sprayed mono-modal coatings (Fig. 10). Despite the use of granules constituted by submicrometric (for Oerlikon-Metco) and nanometric particles (for those agglomerated in the laboratory), the enthalpy of the flame (5223 J/s) used to spray these coatings was excessive for retaining the fine particles in the structures of the samples.

The cumulative distribution functions for the microhardness values of the coatings with changes in the Weibull modulus are shown in Fig. 11, which reveals a bi-modal behavior which is related to the well and partially melted zones in the structures of the coatings, as has been established previously by other authors [4,46–50]. The microhardness values for conventional mono-modal coatings, as well as those calculated from the rule of mixtures for the bi-modal structured samples, are presented in Table 3.

As is evident in Table 3, the microhardness of the PML of the coatings fabricated from Oerlikon-Metco agglomerated and sintered powders is higher than that of the FML, which is due to the α-Al<sub>2</sub>O<sub>3</sub> retained in the PML and the highly cohesive submicrometric particles constituting these zones. The retention of α-Al<sub>2</sub>O<sub>3</sub> in the PML has been reported previously [51]. This phase is harder than the γ-Al<sub>2</sub>O<sub>3</sub> present in the FML [51,52]. On the other hand, in the coatings fabricated from

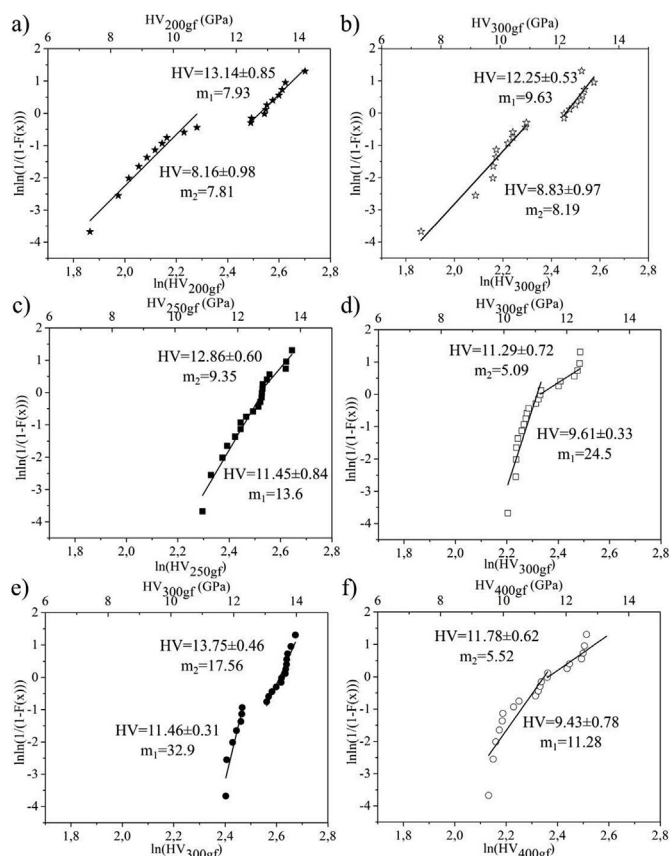


Fig. 11. Weibull plots for the Vickers microhardness values of the bi-modal structured coatings fabricated from different powders. a) Oerlikon-Metco 6103™ spray dried and sintered, b) Oerlikon-Metco 6221™ spray dried and sintered, c) alumina spray dried in the laboratory without sintering, d) AT-13 spray dried in the laboratory without sintering, e) alumina pelletised in the laboratory without sintering, f) AT-13 pelletised in the laboratory without sintering.

pelletised and spray-dried powders which were not sintered, the hardness of the PML is lower than that of the FML, because the fine particles constituting these partially melted zones exhibit poor cohesion between themselves.

#### 4. Conclusions

Alumina and titania nanopowders were agglomerated using an alternative drum pelletisation method to obtain granules of Al<sub>2</sub>O<sub>3</sub>, Al<sub>2</sub>O<sub>3</sub>-13 wt% TiO<sub>2</sub> and TiO<sub>2</sub> which were dried and sieved. The flowability of pelletised granules and their ability to develop bi-modal structures in flame thermal spraying coatings were evaluated and compared with those of granules spray dried with and without sintering, as well as with those for alumina atomised particles blended with TiO<sub>2</sub> granules.

The results indicate that drum pelletisation allows us to obtain micro-sized, spherical-shaped and compact granules, with free-flowing, which are similar to those obtained by spray drying with or without sintering. Although the pelletised granules exhibit sufficient mechanical resistances for transport and thermal spraying, when they come in contact with harder particles like atomised alumina, they can be disintegrated, which decreases their flowability.

The fact that compact and mechanically resistant granules can be obtained by drum pelletisation without sintering to prevent the growth of the fine particles constituting them, which improves the melting ability of these granules in an oxyacetylene flame, makes it possible to use them as feedstock in the fabrication of flame-sprayed coatings.

Drum pelletisation is a suitable method of agglomerating

**Table 3**  
Summary of results obtained from Weibull distribution plots and the microhardness.

| Coatings    |                    | H <sub>PML</sub> | f <sub>PML</sub>                | H <sub>FML</sub> | f <sub>FML</sub> | Microhardness (GPa) |
|-------------|--------------------|------------------|---------------------------------|------------------|------------------|---------------------|
| Pelletised  | A <sub>p</sub>     | 11.46 ± 0.31     | 0.12                            | 13.75 ± 0.46     | 0.88             | 13.49 ± 0.55        |
|             | AT-13 <sub>p</sub> | 9.43 ± 0.78      | 0.09                            | 11.78 ± 0.62     | 0.91             | 11.55 ± 0.99        |
|             | T <sub>p</sub>     |                  | Mono-modal behavior of hardness |                  |                  | 6.03 ± 1.57         |
| Spray dried | AT0 <sub>s</sub>   | 11.45 ± 0.84     | 0.15                            | 12.86 ± 0.60     | 0.85             | 12.65 ± 0.33        |
|             | AT13 <sub>s</sub>  | 9.61 ± 0.33      | 0.13                            | 11.29 ± 0.72     | 0.87             | 11.08 ± 0.79        |
|             | T <sub>s</sub>     |                  | Mono-modal behavior of hardness |                  |                  | 5.22 ± 2.56         |
| Commercial  | A <sub>c</sub>     | 13.14 ± 0.85     | 0.32                            | 8.16 ± 0.98      | 0.68             | 9.75 ± 1.29         |
|             | AT-13 <sub>c</sub> | 12.25 ± 0.53     | 0.56                            | 8.83 ± 0.97      | 0.44             | 10.75 ± 1.11        |
|             | T <sub>c</sub>     |                  | Mono-modal behavior of hardness |                  |                  | 6.23 ± 6.04         |
| Blended     | AT-13 <sub>b</sub> |                  | Mono-modal behavior of hardness |                  |                  | 11.1 ± 2.30         |

H<sub>PML</sub>, Hardness of partially melted lamellae; f<sub>PML</sub>, fraction of partially melted lamellae.

H<sub>FML</sub>, Hardness of fully melted lamellae; f<sub>FML</sub>, fraction of fully melted lamellae.

nanoparticles, with low water and energy consumptions; the agglomerates can be used as feedstock for thermally sprayed coatings, even for those of alumina, which are difficult to flame spray, to obtain a bi-modal yet compact structure.

According to the aforementioned details, drum pelletisation is an alternative method which can replace the spray drying and sintering processes and is frequently used in the preparation of granules which are used as raw materials in the fabrication of bi-modal structured coatings.

### Acknowledgements

The authors are grateful to FONDO NACIONAL DE FINANCIAMIENTO PARA LA CIENCIA, LA TECNOLOGÍA Y LA INNOVACIÓN “FRANCISCO JOSÉ DE CALDAS” COLCIENCIAS, for supporting the projects grant numbers: FP44842-302-2016, FP44842-124-2017 and CT-657-2018.

### References

- P.L. Fauchais, J.V.R. Heberlein, M.I. Boulos, *Thermal Spray Fundamentals from Powder to Part*, Ilustrada, Springer US, Boston, MA, 2012, <https://doi.org/10.1007/978-0-387-68991-3>.
- L. Pawlowski, Finely grained nanometric and submicrometric coatings by thermal spraying: a review, *Surf. Coating. Technol.* 202 (2008) 4318–4328, <https://doi.org/10.1016/j.surfcoat.2008.04.004>.
- R.S. Lima, B.R. Marple, Thermal spray coatings engineered from nanostructured ceramic agglomerated powders for structural, thermal barrier and biomedical Applications: a review, *Therm. Spray Technol.* 16 (2007) 40–63, <https://doi.org/10.1007/s11666-006-9010-7>.
- L. Wang, Y. Wang, X.G. Sun, J.Q. He, Z.Y. Pan, C.H. Wang, Microstructure and indentation mechanical properties of plasma sprayed nano-bimodal and conventional ZrO<sub>2</sub>-8wt%Y<sub>2</sub>O<sub>3</sub> thermal barrier coatings, *Vacuum* 86 (2012) 1174–1185, <https://doi.org/10.1016/j.vacuum.2011.10.029>.
- S.R. Bakshi, V. Singh, S. Seal, A. Agarwal, Aluminum composite reinforced with multiwalled carbon nanotubes from plasma spraying of spray dried powders, *Surf. Coating. Technol.* 203 (2009) 1544–1554 <https://doi.org/10.1016/j.surfcoat.2008.12.004>.
- Oxide Ceramic Powder Materials for Thermal Spray*, (2018).
- Thermal Spraying with Molybdenum Powders*, (2018).
- Sprayable Nanostructured Alumina/Titania S2613S Nanox™ Powder*, (2018).
- J.R. Davis, *Handbook of Thermal Spray Technology*, ASM Intern, USA, 2004.
- H. Herman, Powders for thermal spray technology, *KONA Powder Part. J.* 9 (1991) 187–199, <https://doi.org/10.14356/kona.1991024>.
- X.Q. Cao, R. Vassen, S. Schwartz, W. Jungen, F. Tietz, D. Stöver, Spray-drying of ceramics for plasma-spray coating, *J. Eur. Ceram. Soc.* 20 (2000) 2433–2439, [https://doi.org/10.1016/S0955-2219\(00\)00112-6](https://doi.org/10.1016/S0955-2219(00)00112-6).
- S. Fazio, J. Guzmán, M.T. Colomer, A. Salomoni, R. Moreno, Colloidal stability of nanosized titania aqueous suspensions, *J. Eur. Ceram. Soc.* 28 (2008) 2171–2176, <https://doi.org/10.1016/j.jeurceramsoc.2008.02.017>.
- B. Faure, J. Sæderup Lindeløv, M. Wahlberg, N. Adkins, P. Jackson, L. Bergström, Spray drying of TiO<sub>2</sub> nanoparticles into redispersible granules, *Powder Technol.* 203 (2010) 384–388, <https://doi.org/10.1016/j.powtec.2010.05.033>.
- D.E.E. Walton, C.J.J. Mumford, The morphology of spray-dried particles, *Chem. Eng. Res. Des.* 77 (1999) 442–460, <https://doi.org/10.1205/026387699526296>.
- R. Mondragón, J.E. Julia, A. Barba, J.C. Jarque, El proceso de secado por atomización: formación de gránulos y cinética de secado de gotas, *Bol. La Soc. Esp. Ceram. y Vidr.* 52 (2013) 159–168, <https://doi.org/10.3989/cyv.212013>.
- M. Vicent, E. Sánchez, A. Moreno, R. Moreno, Preparation of high solids content nano-titania suspensions to obtain spray-dried nanostructured powders for atmospheric plasma spraying, *J. Eur. Ceram. Soc.* 32 (2012) 185–194 <https://doi.org/10.1016/j.jeurceramsoc.2011.08.007>.
- M. Vicent, E. Sánchez, I. Santacruz, R. Moreno, Dispersion of TiO<sub>2</sub> nanopowders to obtain homogeneous nanostructured granules by spray-drying, *J. Eur. Ceram. Soc.* 31 (2011) 1413–1419, <https://doi.org/10.1016/j.jeurceramsoc.2011.01.026>.
- P. Roy, G. Bertrand, C. Coddet, Spray drying and sintering of zirconia based hollow powders, *Powder Technol.* 157 (2005) 20–26 <https://doi.org/10.1016/j.powtec.2005.05.031>.
- L. Pawlowski, *The Science and Engineering of Thermal Spray Coatings*, (2008).
- A. Stunda-Zujeva, Z. Irbe, L. Berzina-Cimdirina, Controlling the morphology of ceramic and composite powders obtained via spray drying – a review, *Ceram. Int.* 43 (2017) 11543–11551, <https://doi.org/10.1016/j.ceramint.2017.05.023>.
- G. Bertrand, C. Filiatre, H. Mahdjoub, A. Foissy, C. Coddet, Influence of slurry characteristics on the morphology of spray-dried alumina powders, *J. Eur. Ceram. Soc.* 23 (2003) 263–271, [https://doi.org/10.1016/S0955-2219\(02\)00171-1](https://doi.org/10.1016/S0955-2219(02)00171-1).
- A. Stunda-Zujeva, V. Stepanova, L. Berzina-Cimdirina, Effect of spray dryer settings on the morphology of illite clay granules, *Environ. Technol. Resour. Proc. Int. Sci. Pract. Conf.* 1 (2015) 216–222, <https://doi.org/10.17770/etr2015vol1.200>.
- G. Bertrand, P. Roy, C. Filiatre, C. Coddet, Spray-dried ceramic powders: a quantitative correlation between slurry characteristics and shapes of the granules, *Chem. Eng. Sci.* 60 (2005) 95–102, <https://doi.org/10.1016/j.ces.2004.04.042>.
- J. Lister, B. Ennis, *Tumbling granulation*, *Sci. Eng. Granulation Process. Part. Technol. Ser.*, Springer, Dordrecht, 2004, [https://doi.org/10.1007/978-94-017-0546-2\\_8](https://doi.org/10.1007/978-94-017-0546-2_8).
- A. Levy, H. Kalman (Eds.), *Handbook of Powder Technology* *ume 10* (2001).
- K. Sastry, P. Dontula, C. Hosten, Investigation of the layering mechanism of agglomerate growth during drum pelletization, *Powder Technol.* 130 (2003) 231–237, [https://doi.org/10.1016/S0032-5910\(02\)00271-1](https://doi.org/10.1016/S0032-5910(02)00271-1).
- W. Pietsch, *Agglomeration in Industry: Occurrence and Applications*, Wiley-VCH, Weinheim, 2005.
- M. Rhodes, *Introduction to Particle Technology*, 2da ed., (1998).
- A. Salman, J. Hounslow, J. Seville (Eds.), *Handbook of Powder Technology*, *ume 11 Granulation*, 2007.
- ASTM D1200-10, Standard test method for viscosity by Ford, *Viscosity Cup 10* (2014) 1–4, <https://doi.org/10.1520/D1200-10R18.2>.
- ASTM E1920-03, *Standard Guide for Metallographic Preparation of Thermal Sprayed Coatings*, (2003), pp. 1–5.
- ASTM C1327 15, Standard Test Method for Vickers Indentation Hardness of Advanced Ceramics, Test, (2003), pp. 1–10, <https://doi.org/10.1520/C1327-08.2>.
- H. Zhou, F. Li, B. He, J. Wang, B. de Sun, Air plasma sprayed thermal barrier coatings on titanium alloy substrates, *Surf. Coating. Technol.* 201 (2007) 7360–7367, <https://doi.org/10.1016/j.surfcoat.2007.02.010>.
- N. Orlovskaja, H. Peterlik, M. Marczewski, K. Kromp, The validity of Weibull estimators-experimental verification, *J. Mater. Sci.* 32 (1997) 1903–1907, <https://doi.org/10.1023/A:1018521310570>.
- C.K. Lin, C.C. Berndt, Statistical analysis of microhardness variations in thermal spray coatings, *J. Mater. Sci.* 30 (1995) 111–117, <https://doi.org/10.1007/BF00352139>.
- D.E. Walton, The morphology of spray-dried particles a qualitative view, *Dry. Technol.* 18 (2000) 1943–1986, <https://doi.org/10.1080/07373930008917822>.
- E. Sánchez, A. Moreno, M. Vicent, M.D. Salvador, V. Bonache, E. Klyatskina, I. Santacruz, R. Moreno, Preparation and spray drying of Al<sub>2</sub>O<sub>3</sub>-TiO<sub>2</sub> nanoparticle suspensions to obtain nanostructured coatings by APS, *Surf. Coating. Technol.* 205 (2010) 987–992, <https://doi.org/10.1016/j.surfcoat.2010.06.002>.
- E. Hadjittofis, S.C. Das, G.G.Z. Zhang, J.Y.Y. Heng, *Interfacial Phenomena*, Elsevier Inc., 2016, <https://doi.org/10.1016/B978-0-12-802447-8.00008-X>.
- L.A. Shervington, A. Shervington, *Analytical profiles of drug substances and excipients*, *Jordanian Pharm. Manuf. Med. Equip. Co. Ltd.* 25 (1998) 121–164.
- M. Vicent, E. Bannier, R. Moreno, M.D. Salvador, E. Sánchez, Atmospheric plasma spraying coatings from alumina-titania feedstock comprising bimodal particle size distributions, *J. Eur. Ceram. Soc.* 33 (2013) 3313–3324, <https://doi.org/10.1016/j.jeurceramsoc.2013.05.009>.
- X. Lin, Y. Zeng, S.W. Lee, C. Ding, Characterization of alumina-3 wt.% titania coating prepared by plasma spraying of nanostructured powders, *J. Eur. Ceram.*



- Soc. 24 (2004) 627–634, [https://doi.org/10.1016/S0955-2219\(03\)00254-1](https://doi.org/10.1016/S0955-2219(03)00254-1).
- [42] R. McPherson, On the formation of thermally sprayed alumina coatings, *J. Mater. Sci.* 15 (1980) 3141–3149, <https://doi.org/10.1007/BF00550387>.
- [43] E. Cadavid, C. Parra, F. Vargas, Estudio de llamas oxiacetilénica usadas en la proyección térmica, *Rev. Colomb. Mater.* (2016) 15–26.
- [44] P. Boch, J.-C. Niépce, *Ceramic Materials Processes, Properties and Applications*, ISTE Ltd, United States, 2007, <https://doi.org/10.1002/9780470612415>.
- [45] L.E. Oi, M.Y. Choo, H.V. Lee, H.C. Ong, S.B.A. Hamid, J.C. Juan, Recent advances of titanium dioxide (TiO<sub>2</sub>) for green organic synthesis, *RSC Adv.* 6 (2016) 108741–108754, <https://doi.org/10.1039/c6ra22894a>.
- [46] F.M. Hurtado, A.G. Hernández, M.E.L. Gómez, H. Ageorges, Estudio de la estructura y las propiedades mecánicas en un recubrimiento de circona estabilizada con 8% en mol de itria elaborado por proyección térmica por plasma a partir de suspensiones, *Matéria (Rio Janeiro)* 21 (2016) 49–60, <https://doi.org/10.1590/S1517-707620160001.0005>.
- [47] Y. Zhao, Y. Gao, Deposition of nanostructured YSZ coating from spray-dried particles with no heat treatment, *Appl. Surf. Sci.* 346 (2015) 406–414, <https://doi.org/10.1016/j.apsusc.2015.03.164>.
- [48] R.S. Lima, A. Kucuk, C.C. Berndt, Bimodal distribution of mechanical properties on plasma sprayed nanostructured partially stabilized zirconia, *Mater. Sci. Eng. A* 327 (2002) 224–232, [https://doi.org/10.1016/S0921-5093\(01\)01530-1](https://doi.org/10.1016/S0921-5093(01)01530-1).
- [49] H. Wang, J. Ma, G. Li, J. Kang, B. Xu, The dependency of microstructure and mechanical properties of nanostructured alumina – titania coatings on critical plasma spraying parameter, *Appl. Surf. Sci.* 314 (2014) 468–475, <https://doi.org/10.1016/j.apsusc.2014.07.026>.
- [50] J. Kang, J. Ma, G. Li, H. Wang, B. Xu, C. Wang, Bimodal distribution characteristic of microstructure and mechanical properties of nanostructured composite ceramic coatings prepared by supersonic plasma spraying, *Mater. Des.* 64 (2014) 755–759, <https://doi.org/10.1016/j.matdes.2014.08.038>.
- [51] A. Rico, J. Rodríguez, E. Otero, P. Zeng, W.M. Rainforth, Wear behaviour of nanostructured alumina-titania coatings deposited by atmospheric plasma spray, *Wear* 267 (2009) 1191–1197, <https://doi.org/10.1016/j.wear.2009.01.022>.
- [52] T.C. Chou, T.G. Nieh, S.D. McAdams, G.M. Pharr, Microstructures and mechanical properties of thin films of aluminum oxide, *Met. Mater.* 25 (1991) 2203–2208.